

Transitioning from shear to flexural failure of Ultra High Performance Concrete Beams by varying fiber content

Shady Goma¹ , Mohammed Alnaggar²

Authors & Affiliation:

¹ PhD Candidate, Department of Civil and Environmental Engineering, Rensselaer Polytechnic Institute, 110 8th St, Troy, NY 12180 USA. E-mail: gomaas3@rpi.edu

² Assistant Professor, Department of Civil and Environmental Engineering, Rensselaer Polytechnic Institute, 110 8th St, Troy, NY 12180 USA. E-mail: alnagm2@rpi.edu

Abstract:

Ultra High Performance Concrete (UHPC) is a new class of cementitious materials that has been developed recently. Compared to normal reinforced concrete, it has very high compressive strength, durability, and long-term stability. However, the presence of high volumetric content of fibers along with the very small maximum aggregate size set its behavior apart from both regular and fiber reinforced concrete, especially in shear.

While many experimental campaigns were directed towards understanding UHPC beams behavior, those which considered shear failure were mostly performed by using beams with non-rectangular cross sections. This limits the applicability of their findings in other cases. In addition, many tests did not track the the effects of including fibers compared to having no fibers at all. In this study, an experimental campaign was performed which included twelve reinforced prismatic UHPC beams in addition to multiple companion specimens for characterizing the material properties. Fiber volumetric contents were 0%, 1% and 2%. Rebar reinforcement was either one or two #3 Grade 60 rebars. Beams were 3 in x4 in (76 mm x 101.5 mm) in cross section and were tested in 3 point bending setup over 18 in (457 mm) span. For each fiber content, splitting tension, compression and notched 3 point bending tests were performed to characterize the material strength. Beam testing showed a transition from diagonal shear failure at 0% fiber content to full rebar rupture at 2% fiber content. At 1% fiber content, very small diagonal shear cracks were observed with 2 rebars but not with 1 rebar, yet, fiber crack bridging prevented the development of critical shear cracks. Results show an interplay between reinforcement ratio and fiber content that is not a simple addition of their individual effects which calls for considering their effects on strength and ductility in a coupled manner.

Keywords:

Reinforce UHPC beams, Diagonal Shear, Fiber crack bridging

1. Introduction

Ultra High Performance Concrete (UHPC) is class of cementitious materials with superior strength, ductility and durability [Graybeal 2006]. Its mechanical behavior has been the subject of many experimental studies to characterize its suitability for different applications. Use of UHPC in bridges is of special interest, and thus, many experimental campaigns tested its flexural behavior but less ones focused specifically on its shear behavior. Flexural capacity studies on UHPC beams included different reinforcing rebars ratios with 2% fiber content [Yang et al. 2010]. Changing fiber shape (hooked and crimped) and fiber content (by volume) has been studied on square cross-section UHPC beams [Khalil and Tayfur 2013]. Singh et al. [Singh et al. 2017] performed an experimental work to study the flexural behaviour of prismatic UHPC beams with different spans and reinforcement. Shear capacity was also studied but mostly with beams that have non-rectangular cross sections. 11 Ultra High Performance Fiber Reinforced Concrete (UHPFRC) girders with A-Type cross-section were tested under shear and simplified formulations for the first cracking load were proposed [Wu and Han 2009]. Voo et al. [Voo et al. 2010] tested 8 prestressed UHPC girders also with A-type cross-sections. Xia et al. [Xia et al. 2011] studied T-section UHPC beams reinforced with high strength steel (HSS) rebars. Yang et al. [Yang et al. 2012] performed a shear capacity experimental study on 12 I-shape UHPC beams with longitudinal reinforcements and without stirrups. Wahba et al. [Wahba et al. 2012] designed an experimental program to test the shear failure of 5 UHPC beams without stirrups in 4 point bending setup having shear span ratios of $a/d = 2.3$ and 4.6 , however all beams failed in flexure. Qi et al. [Qi et al. 2016] performed an experimental study on shear strength of eleven T-section HSS-UHPFRC with longitudinal and transverse reinforcement and $a/d = 3.17$. The shear behavior of UHPFRC I-shaped beams with and without web opening has been also studied [Zagon et al. 2016]. Additionally, effects of varying shear reinforcement were studied using beams ($a/d=3$) with rectangular cross sections and fiber volume fraction of 1.5% [Lim and Hong 2016]. Pourbaba et al. [Pourbaba et al. 2018] performed an experimental comparison between UHPFRC rectangular beams and normal reinforced concrete under shear with varying a/d (0.8, 1.2 and 2.8) and reinforcement ratio (2.2% to 7.8%). Chen et al. [Chen et al. 2018] planned also to study combined Shear and bending of rectangular UHPC beams with varying fiber contents under three point bending setup, but all beams failed in bending. A successful experimental study on shear behavior of I-shaped UHPC beams with steel reinforcement was recently reported [Mészöly and Randl 2015].

As it can be seen from literature, most of the experimental studies performed to understand shear behaviour of the UHPC beams were carried using non-rectangular sections. It can be also seen that most of the ones performed using rectangular sections failed in bending. Therefore, the focus of this study is to provide a smooth transition from shear to bending failure as a function of increasing fibers content. In addition, the current study shows the interplay between fiber content and reinforcement ratio and their effects on peak load and ductility.

2. Materials and Experiments

An experimental program was designed to characterize the contribution of short metal fibers, used traditionally in UHPC formulations, to the load carrying capacity and mode of failure change of reinforced UHPC prismatic beams in 3 point bending. A total of 12 beams were prepared along with corresponding companion specimens to identify the material strength. The UHPC mix used

was donated by Ductal[®]. The proprietary mix contains: 58.87 lb/ft³ (943 kg/m³) of binder materials with 0.138 of Water-to-binder ratio and 1.305 of fine aggregate-to-binder ratio. The maximum aggregate size is 0.024 in (0.6 mm). Fiber used are Dramix[®] steel fibers with 0.008 in (0.2 mm) diameter and 0.5 in (12.7 mm) length. A High range water reducer was used at a dose of 2.12 lb/ft³ (34 kg/m³). Longitudinal steel reinforcement used for the beams were #3 Grade 60 rebars. A total of 3 batches were made. All batches had exactly the same components except the fibers content which was 0%, 1%, and 2% for the first, second and third batch, respectively. Each batch was used to cast a total of 4 beams and their corresponding companion specimens. A 1.5 HP high shear horizontal mixer (Collomix XM-2/650) was used for mixing which allowed for a short mixing cycle and improved homogeneity. Dry premix was mixed for 2-4 minutes. during that time, the superplasticiser dose was added to water and thoroughly mixed. Mixed water is then added gradually to the premix while the mixer is running over a period of 3-5 minutes. Mixing is then continued uninterrupted for at least 5 minutes more. Finally, for mixes with fibers, while the mixer is running, the fibers are gradually fed through a top whole withing 3-5 minutes. Finally, the batch was mixed for another 5 minutes to achieve homogeneous fiber distribution. The static flow test was performed on the mix without fibers and an average flow of 8.09 in (205.5 mm) was achieved. Cast samples are all covered with tight plastic wrap and left in molds for 30±1 hours in room temperature. Next, samples were demolded and then moved into a water curing tank with controlled temperature of 80.6° F (27° C) . Curing continued for 90±2 days. For each batch, material strength was characterized by performing unconfined compression, brazilian splitting and notched 3 point bending tests. In addition, reinforced beams from each batch were also tested in 3 point bending to characterize their structural behavior and mode of failure. Tests details were as follows:

2.1 Companion specimens tests

Unconfined compression tests were performed by using cubic specimens with 2 in (50.8 mm) of edge length. Low friction at loading surfaces was introduced by inserting two Teflon sheets between sample surfaces and loading platens. The top platen had a swiveling head. Cubic samples were also specifically chosen over US standard cylindrical samples to maximize surface flatness and to make sure both surfaces were parallel. Loaded surfaces were those facing the mold sides and thus no treatment was needed. For each tested sample, all twelve cube edges are measured using a caliper with 0.00004 in (0.001 mm) accuracy. Average cross-sectional area as well as average cube height were then calculated to be used for test results post-processing. An Instron 5950 universal testing machine with 300 kip (1,300 kN) capacity was used to perform the test. Loading rate was constantly held at 0.1 in/min (2.54 mm/min) across the whole test period which resulted in 30 to 40 psi/s (0.20 to 0.28 MPa/s) stress rate during elastic loading.

Brazilian splitting tests were performed by using cylindrical samples with nominal dimensions of 2 in (50.8 mm) diameter and 4 in (101.6 mm) height. Since all samples were cast in plastic molds of 4 in (101.6 mm) height, the top part contained some bubbling and had to be cut to guarantee a clear surface. To get uniform cutting using a wet circular tile saw, a relatively thick slice had to be cut and that shortened the tested samples by about 0.5 in (12.5 mm). Two steel prismatic rods with square cross sections having 0.25 in (6.35) mm edge length were used to apply the line loads on the cylinder edges. The top loading assembly was held against the top swiveling head of the same Instron machine used for compression testing via rubber bands. The loading rate was also held con-

stant across the whole test period at 0.1 in/min (2.54 mm/min). Cylinder diameter was measured at top, center and bottom along between the two loading lines marks. Also, cylinder height was measured along both loading line marks. The average diameter and average height were used in results post-processing. The use of steel rods instead of wooden ones was because previous tests by the research team using wood on similar UHPC samples resulted in creating a secondary crack and thus, large scattering was encountered. But also, the use of steel rods with a small contact width of only 0.25 in (6.35 mm) resulted in a noticeable local damage, especially for the batches with fibers.

Notched 3 point bending tests were performed by using prismatic samples 12 in (305 mm) long with 2 in × 2 in (50.8 mm × 50.8 mm) in cross section. samples were supported simply on a 6 in (152.5 mm) span to have 100% self-weight compensation. A half height notch was made using the same wet circular tile saw. The notch width was 0.12 in (3 mm). Vertical displacement was recorded by measuring the difference between the loading point and the two points above the loading plates. This was done by using 2 digital indicators with 0.001 in (0.002 mm) accuracy. In addition, the Crack mouth opening displacement was also recorded using a CMOD gauge with 0.4 in (10 mm) gauge length. An MTS 810 universal testing machine was used with a 55 kip (250 kN) load cell. Loading was controlled using very slow stroke displacement of 0.001 in/min (0.025 mm/min). It should be emphasized here that the correct method of control should be CMOD control but due to problems with the calibration of PID control parameters, multiple test trials failed to achieve good control using the CMOD, therefore, the stroke displacement was used. Drawbacks of this control mode are discussed in the results section.

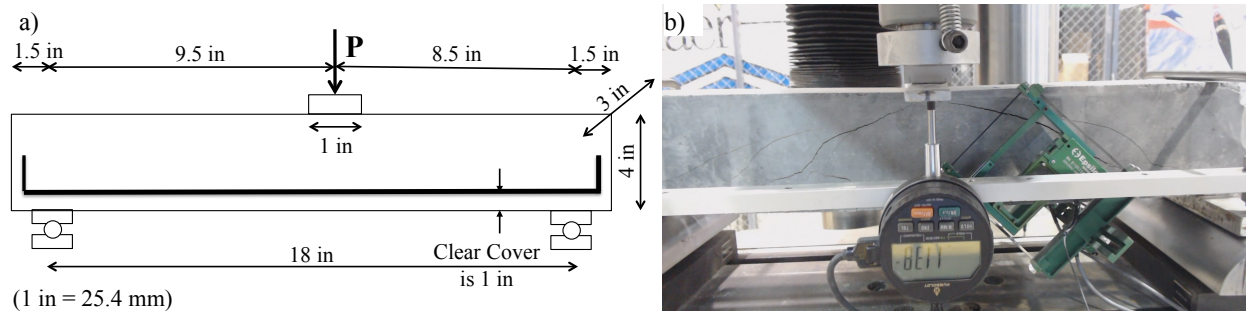


Figure 1: a) UHPC beams dimensions and test setup, b) Deflection and crack measurement

2.2 Reinforced UHPC beams 3 point bending test

To study the interplay of reinforcement ratio and fiber content on reinforced UHPC beams capacity and mode of failure under 3 point bending loading. Four beams per each of the three batches were tested. Two beams were reinforced by a single #3 rebar and the other two were reinforced with two #3 rebars. Rebars were Grade 60 steel. The dimensions and reinforcement details of the tested beams are shown in Figure 1a. Beam length was 21 in (533 mm) with a simply supported span of 18 in (457 mm). The point load was made intentionally eccentric by 0.5 in (12.7 mm) from the center line of the beam to produce an unequal shear force. By doing so, an averaging extensometer was installed on both beam sides (across its thickness) perpendicular to the expected main shear crack to measure its opening for cases where shear cracks would develop (see Figure

1b). The clear bottom cover was 1 in (25.4 mm). It was intentionally made large to facilitate fibers flow around the rebars and to prevent any possible lower cover spalling. Steel plates were used to reduce friction between the beams and the supports. In addition, two digital indicators were supported on a suspension system that rests exactly on top of the beam above both supports. The indicators plungers point to the point load steel plate. The average reading of the two indicators was used to determine the vertical deflection. Load was applied using the same 300 kips (1,300 kN) Instron machine at a rate of 0.1 in/min (2.54 mm/min). Details of the averaging extensometer and vertical deflection measuring apparatus are shown in Figure 1b.

3. Results and Discussion

3.1 Material strength characterization

Unconfined compression strength: For each batch, six cubic specimens were tested. Figures 2a-c show both the average and envelopes of the engineering stress-strain curves for each batch (0%, 1% and 2% fiber content). Similarly to previous research campaigns, the compressive strength of the plain UHPC mix is typically smaller than the same material with fibers due to the added interlocking and confinement from fibers. As can be seen from results, the plain UHPC batch had an average $f'_c = 17.5$ ksi (120.53 MPa). By adding fibers, f'_c reached the expected range of this UHPC material. It can be noticed that the fiber content has no significant effects on the average peak strength ($f'_c = 22.2$ ksi = 152.97 MPa for 1% fiber content and 21.2 ksi = 146.04 MPa for 2% fiber content). Additionally, the scatter of the 1% fiber case is higher than the 2% case. Furthermore, one can notice a slight increase in the toughness of the 2% fiber case compared to the 1% case by comparing the areas under the two curves, yet it is not very clear. As discussed earlier, Teflon sheets provided a very low friction condition at both sides of the cubes which guaranteed a full vertical splitting failure of all specimens. These results attest to the robustness of this procedure to evaluate compressive strength with much less effort in sample preparation and post processing.

Splitting Tensile Strength: Brazilian splitting tests of six cylinders per each batch were performed. Average and envelopes of engineering stress versus vertical strain defined as the machine stroke divided by the sample diameter are shown in Figures 2d-f. The addition of fibers increases f_{sp} as expected. For the two batches with fibers, a clear kink around 15 MPa is observed in the curves. At this point, the top thin steel loading platen penetrates partially the top surface of the cylinder as it compresses the damaged cracked area under it. It is believed that this is the reason why indirect splitting tensile strength is not a good measure for UHPC's tensile strength since this local damage redistributes the stresses and creates a plastic damage zone around it.

Flexural tensile strength: Notched 3 point bending tests were performed. It must be emphasized here that the tensile strength f_r computed from this test is not the standard tensile strength of the material due to the continuous changing of the neutral axis location and the effect of fiber contribution. Yet, one can use the results from this test to indirectly calculate the tensile strength f'_t (see [Amin et al. 2018]). Average and envelopes of nominal stress versus nominal strain are shown in in Figures 2g-i. Nominal stress is calculated as $\sigma_f = 3PL/2bh^2$ where P is load, and L , b , and h are effective span, width, and depth of the specimen respectively; while nominal strain is calculated as $\epsilon_f = CMOD/h$. For 0% fiber content, one of the two tested samples partially cracked

during notch cutting, therefore, only one result is available. For the two other cases, two samples were tested and both had very close results as can be seen from Figures 2 h&i. Generally, presence of fibers and their content has a large effect on ductility, peak capacity and toughness.

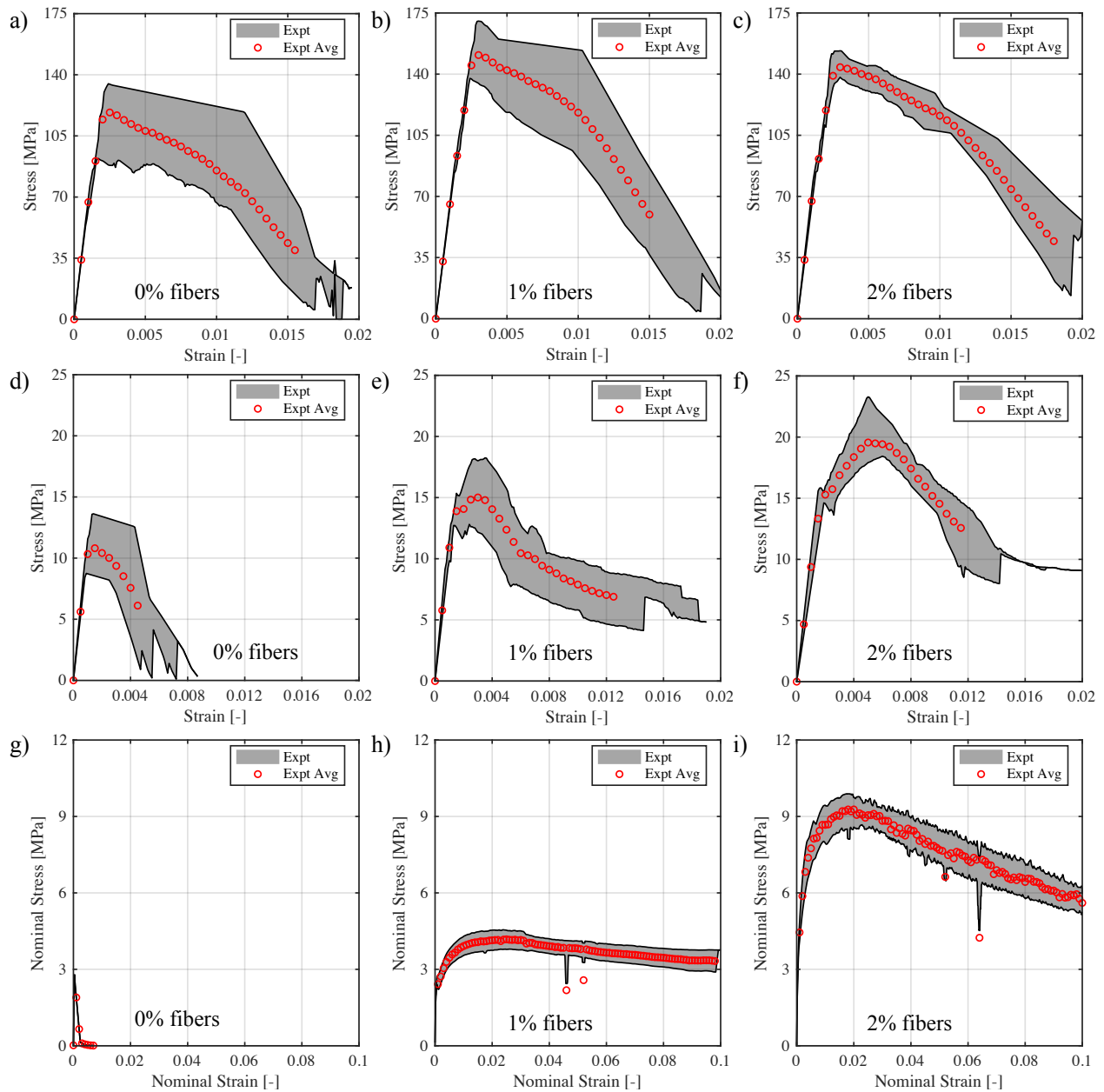


Figure 2: Stress versus strain curves of companion specimens under: a-c) Uniaxial compression, d-f) Splitting tension, and g-i) Notched 3 point bending tests (1 MPa = 145 psi)

3.2 Reinforced UHPC beams test results

Load versus loaded point displacement results as well as the failure patterns of the tested beams are shown Figure 3. For each batch/reinforcement case, the two tested beams envelopes are plotted along with their average. Average peak loads of each two beam replica, beam dimensions and

reinforcement details are also listed in Table 1. By comparing the results, multiple interesting mechanisms can be inferred.

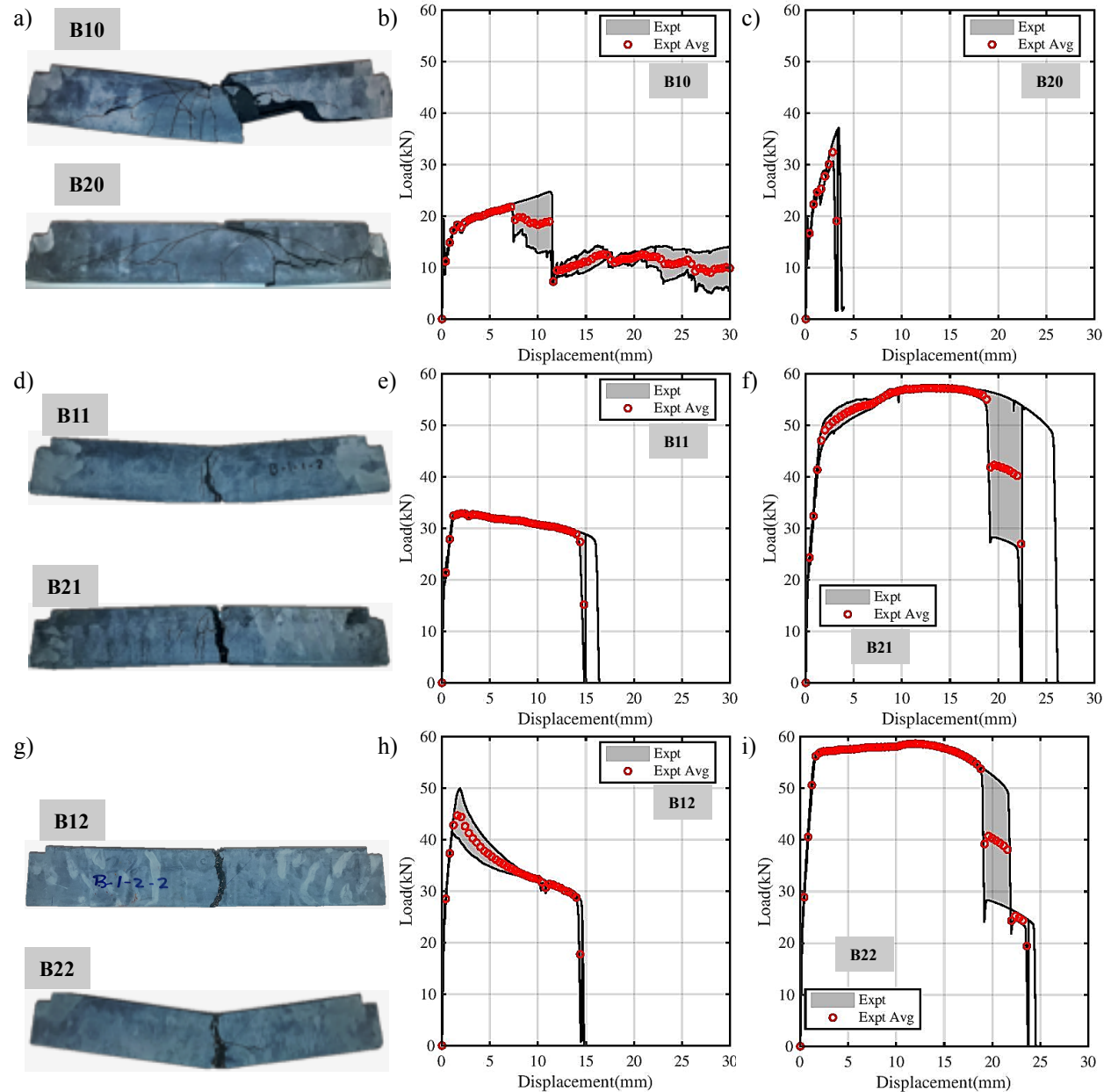


Figure 3: Failure modes and load-displacement responses of reinforced UHPC beams under 3 point bending test (25.4 mm = 1 in, 1 kN = 225 lb)

At 0% fiber (Figures 3a-c), a clear brittle shear failure develops in both reinforcement levels (single and double rebars). But by careful analysis of the ductility, one can see that the single rebar case (B10) shows a much larger ductility and a lower capacity. This result indicates that the rebars were stressed beyond their elastic limit and there is a possibility of yielding and strain hardening before the beam reaches its shear capacity. To check this assumption, The bending capacity of the two beams is calculated using general reinforced concrete bending capacity following ACI-

318-14 [ACI-318-14 2014]. Material parameters used in the calculations are: $E_c = 8700$ ksi (60 GPa) (calculated from notched 3 point bending test), $f'_c = 17.4$ ksi (120 MPa), $E_s = 29000$ ksi (200 GPa), and $f_y = 69.6$ ksi (480 MPa) (from rebar tension tests not included in this paper due to length limitations). Beam section is 3 in \times 3.4 in (76 mm \times 86.5 mm). These parameters give $M_n = 1.22$ kip.ft (1.66 kN.m) for B10 which corresponds to a peak load $P_n = 3.64$ kip (16.2 kN). This is where the slope tends to clearly change in Figure 3b. Thus, the shear failure of B10 is triggered after rebar yielding due to the continued strain hardening of the rebars. This explains why B20 carried higher loads. By calculating its bending capacity, one gets $M_n = 2.35$ kip.ft (3.19 kN.m) which corresponds to a peak load of $P_n = 7$ kip (31.1 kN). It is very interesting to see that this capacity is around the measured beam capacity (Figure 3c). This means that the onset of yielding triggered a shear failure. This is also because this very fine and high strength material is fully bonded to the rebar. So, once the rebar starts yielding, it initiates cracks and thus the originally intact UHPC cross section is reduced due to the development of the crack. This means that, since B10 yields at a relatively small load, the cracked UHPC was not sheared until significant yielding advanced and propagated the critical shear cracks up in the shear span. So, for B10, the initiation of shear failure was dependent on crack opening due to continued strain hardening not on the material shear strength. But for B20, the higher capacity induced higher compression in the intact UHPC part which raised its resistance until cracks started to develop but since the load is very high, the UHPC section did fail in shear. This conclusion can be partially supported if we consider the nominal shear strength based on ACI 318-14 [ACI-318-14 2014]. Using the same parameters, $V_c = 3.5$ kip (15.56 kN). While this value is clearly lower than the experimentally measured ones, it is close to the load required to initiate yielding in B10, which means that UHPC was not over-stressed in shear while the rebar was undergoing strain hardening. On the other hand, once the rebars in B20 started to yield, the UHPC was already highly stressed in shear and thus it did fail suddenly. These conclusions are also supported by the cracks on the specimens in Figure 3a. It is clear that B10 shows many small vertical cracks in the middle third which indicates a progressive yielding, while B20 has only 1 crack under the load and it did not even grow much up towards the neutral axis. Nevertheless, both beams eventually show a clear diagonal shear failure. For cases with fibers, there is a clear fiber crack bridging at both levels of fiber contents which resulted in an eventual flexural failure in all the four beam cases (B11, B12, B21 and B22). Yet, the interplay between fiber content and reinforcement is complex and must be explained in a coupled manner. At 1% fiber content, fibers increased the shear capacity noticeably by preventing diagonal cracks from developing/growing. The fibers efficiency was higher with the single rebar case (B11) as can be seen from the cracking patterns in Figure 3d. One can hardly see cracks in the shear span (only one small vertical crack). By preventing cracks, fibers are forcing the single rebar to locally yield, preventing a distributed yielding mechanism. This can be seen clearly from the limited strain hardening zone in Figure 3e. The change from elastic response (up to about 4.05 kip = 18 kN) to localised strain hardening up to the peak is occurring within 0.08 in (2 mm) of deflection only. The beams completely failed and was cut into two pieces with clear necking of the rebar at around 0.59 in (15 mm) to 0.63 in (16 mm). With 2 rebars, the fibers are relatively weaker as a couple of additional vertical cracks are noticed around the loading point (Figure 3d) and are clearly larger than those in B11. Also, 2 small sub-critical diagonal cracks have been formed. This indicates a more distributed yielding which is clearly reflected in the total ductility of B21 failing around 0.9 in (23mm) to 1.02 in (26 mm). Also, a clear strain hardening segment is noticed in the load displacement curve (Figure 3f) where the peak load for B21 occurs at 0.55 in

(14 mm) displacement while the peak load for B11 occurs only at 0.08 in (2 mm). This interplay is more emphasized at 2% fiber content. With 1 rebar, B12 behaves very similarly to B11 but fiber contribution increases its peak capacity (Figure 3h). Nevertheless, since fibers bridge cracks very strongly and even prevent cracks from developing, a steeper post peak slope is observed and B12 fails at 0.57 in (14.5 mm) displacement compared to about 0.59 in (15mm) to 0.63 in (16 mm) with less fibers. So, the increased capacity was at a slight expense of ductility. One can see this when comparing the failure modes of both B11 and B12 in Figures 3d&g. There is a single crack under the load for B12 but one can see some small cracks around the main crack in B11. When 2 rebars are present, B22 behaves similarly to B21. Here, fibers contribution to the strength is nearly negligible because the rebars were undergoing strain hardening while fibers are pulling out in the main crack under the point load. For B21, with 1% fibers, the fiber contribution to the capacity is smaller compared to B22, therefore, the strain hardening curve is more clear and it starts around 11.25 kip (50 kN) and 0.08 in (2 mm) displacement as shown in Figure 3f. Since, B22 has more fibers, their contribution was higher at the beginning of rebar yielding (see Figure 3i), so the strain hardening of the rebars is not as clear and the overall strain hardening behavior starts around 12.6 kip (56 kN) and 0.08 in (2 mm) displacement too. Nevertheless, a main conclusion of this result is that at high reinforcement ratios, fibers content does not significantly affect the ductility or the peak load but it clearly affects the onset of strain hardening. It could also be said that increasing fibers content would increase the load carrying capacity only if the reinforcement ratio is small enough so that fibers can force the reinforcement to locally yield. This means that one can not increase the ductility of a beam by just adding fibers as they can undermine the benefit of having multiple yielding/strain hardening locations along the beam.

Table 1: Peak Loads and Beams Parameters (25.4 mm = 1 in, 1 kN = 225 lb)

Beam ID	A _S	% Fiber	Depth (mm)	width (mm)	Average Peak Load (kN)
B10	1#3	0%	86.39±0.84	76.11±0.70	23.05
B20	2#3	0%	87.36±0.87	76.2±0.32	33.89
B11	1#3	1%	87.66±0.65	76.11±0.70	33.06
B21	2#3	1%	87.66±0.66	76.04±0.11	57.4
B12	1#3	2%	87.24±0.95	76.25±0.02	45.61
B22	2#3	2%	89.05±4.1	76.2±0.05	58.75

4. Conclusions

This paper provide a systematic experimental analysis of reinforced UHPC beams failure with varying reinforcement and fiber contents. Results show a transition from shear failure at 0% fiber content to flexural failure at 2% fiber content. The presence of fibers prevents shear cracks from initiating or developing into critical shear cracks. Evidence of coupling between fiber content and reinforcement was shown which calls for considering their effect in combination not just by additive summation. At the same reinforcement, increasing fibers content improves initial ductility yet, it results in more localized reinforcement yielding and thus, reduced not increased overall ductility. At high reinforcement ratios, increasing fibers content has a slight effect on peak loads. More investigation is needed for diagonal shear failure of rectangular UHPC beams with both reinforcement and different fiber contents, which is currently being pursued by the research team.

References

- ACI Committee 318. (2014). Building Code Requirements for Structural Concrete (ACI 318M-14) and Commentary (318R-14). Farmington Hills, MI: American Concrete Institute.
- Amin, A. , Foster, S. J. and Muttoni, A. "Derivation of the σ -w relationship for SFRC from prism bending tests." *Engineering Structures* 168 (2018): 119-127.
- Chen, Shiming, et al. "Flexural behaviour of rebar-reinforced ultra-high-performance concrete beams." *Magazine of Concrete Research* 70.19 (2018): 997-1015.
- Graybeal, Benjamin A. "Material property characterization of ultra-high performance concrete." No. FHWA-HRT-06-103. 2006.
- Khalil, Wasan I., and Y. R. Tayfur. "Flexural strength of fibrous ultra high performance reinforced concrete beams." *ARNP Journal of Engineering and Applied Sciences* 8.3 (2013): 200-214.
- Lim, Woo-Young, and Sung-Gul Hong. "Shear tests for ultra-high performance fiber reinforced concrete (UHPFRC) beams with shear reinforcement." *International Journal of Concrete Structures and Materials* 10.2 (2016): 177-188.
- Mészöly, Tamás, and Norbert Randl. "Shear behavior of fiber-reinforced ultra-high performance concrete beams." *Structural Concrete* (2015), 16: 93-105. doi:10.1002/suco.201400018
- Pourbaba, Masoud, Abdolreza Joghataie, and Amir Mirmiran. "Shear behavior of ultra-high performance concrete." *Construction and Building Materials* 183 (2018): 554-564.
- Qi, Jia-Nan, et al. "Post-cracking shear strength and deformability of HSS-UHPFRC beams." *Structural Concrete* 17.6 (2016): 1033-1046.
- Singh, M., et al. "Experimental and numerical study of the flexural behaviour of ultra-high performance fibre reinforced concrete beams." *Construction and Building Materials* 138 (2017): 12-25.
- Voo, Yen Lei, Wai Keat Poon, and Stephen J. Foster. "Shear strength of steel fiber-reinforced ultrahigh-performance concrete beams without stirrups." *Journal of structural engineering* 136.11 (2010): 1393-1400.
- Wahba, K., H. Marzouk and N. Dawood. "Structural Behavior of UHPFRC Beams without Stirrups." 3rd International Structural Specialty Conference (2012).
- Wu, Xiangguo, and Sang-Mook Han. "First diagonal cracking and ultimate shear of I-shaped reinforced girders of ultra high performance fiber reinforced concrete without stirrup." *International Journal of Concrete Structures and Materials* 3.1 (2009): 47-56.
- Xia, Jun, et al. "Shear failure analysis on ultra-high performance concrete beams reinforced with

high strength steel.” *Engineering Structures* 33.12 (2011): 3597-3609.

Yang, In Hwan, Changbin Joh, and Byung-Suk Kim. ”Structural behavior of ultra high performance concrete beams subjected to bending.” *Engineering Structures* 32.11 (2010): 3478-3487.

Yang, In-Hwan, Changbin Joh, and Byung-Suk Kim. ”Shear behaviour of ultra-high-performance fibre-reinforced concrete beams without stirrups.” *Magazine of Concrete Research* 64.11 (2012): 979-993.

Zagon, Raul, Stijn Matthys, and Zoltan Kiss. ”Shear behaviour of SFR-UHPC I-shaped beams.” *Construction and building materials* 124 (2016): 258-268.